Magma storage and ascent conditions beneath Pico and Faial islands (Azores archipelago): A study on fluid inclusions

Vittorio Zanon

Centro de Vulcanologia e Avaliação de Riscos Geológicos, Universidade dos Açores, Rua Mãe de Deus, Ponta Delgada, PT-9501-801, Portugal (vittorio.vz.zanon@azores.gov.pt)

Maria Luce Frezzotti

Dipartimento di Scienze Geologiche e Geotecnologie, University of Milan "Bicocca", Milan, Italy

[1] In the islands of Faial and Pico (the Azores), fluid inclusions are hosted in megacrysts of olivine (Mg#80–88) and clinopyroxene (Mg#79–90) in highly porphyritic lavas and in mineral assemblages of ultramafic xenoliths. Rare inclusions are contained in olivine phenocrysts (Mg# < 80) and plagioclases in poorly porphyritic lavas. Trails of late-stage inclusions are predominant over isolated early-stage inclusions. Almost all inclusions are re-equilibrated and the trapped fluid consists of pure CO_2 (Tm from −56.5 to −57.2). Rare early-stage inclusions may contain dypingite or Mg-calcite, which indicates that in earlier times some water was present along with CO_2. Barometric data indicate that CO_2 inclusions in xenoliths from the two islands equilibrated at maximum pressures of 570–586 MPa (19.7–21.2 km), while in poorly porphyritic lavas from all the fissure zones at 465–508 MPa (16.4–18.1 km). Maximum pressure values of 463 MPa (16.8 km) and 492 MPa (17 km) were recorded for the central volcanoes of Pico and Faial, respectively. Further trapping/re-equilibration was recorded at 156 MPa in Faial (5.6 km), in plagioclase phenocrysts in mugearites. All these pressures correspond to magma ponding sites and to its crystallization and can be useful for tracing the progressive thickening of a dense transition zone, below the geophysical Moho. The ability to extract rapidly the stored magmas from these volcanic systems strictly depends on the different tectonic styles, acting in this transition zone. Magmatic evolution in small and short-lived intracrustal reservoirs, not necessarily coaxial with main conduit system, was enhanced at the intersection of differently oriented lineaments.

1. Introduction

[2] Volcanic eruptions in areas characterized by extensional tectonics typically originate from fissure systems, which generally follow local or regional weakness patterns, or from composite volcanoes. Magmas erupted from these systems are characterized by different patterns of evolution, linked to different pathways to the surface [*Klügel et al.*, 2009; *Eason and Sinton*, 2009; *Sigmundsson et al.*, 2010]. Thin mafic lava flows issued from fissure zones constitute the bulk of the erupted material from these volcanoes.

[3] Magma buoyancy plays a major role in the dynamics of magma flow and storage [*Wilson and Head*, 1981], as it controls the depth at which magma reservoirs formed either in the crust or along large lithospheric discontinuities [*Ryan*, 1993; *Ida*, 1995; *McLeod*, 1999]. Magma buoyancy is related to the density difference between host rocks and magma and depends on the pressure, temperature, and composition of both host rocks and magma [*Ryan*, 1994] and also on the tectonic stress [*Watanabe et al.*, 1999].

[4] The study of the geophysical anomalies caused by intruding magma (i.e., seismicity, deformations, and gravity variations), is traditionally used to model the location of the storage system beneath a volcano, the dynamics of magma ascent and the mass involved. However, in the absence of a reliable model for the composition and density of the crust, the application of geophysical methods cannot provide precise information about the location of magma ponding sites, as is the case of the Azores. An alternative way of obtaining the pressure of magma accumulation at various levels consists of a combination of petrological studies on magma evolution, with fluid inclusion barometric studies [e.g., *Roedder*, 1983; *Belkin and De Vivo*, 1993; *Andersen and Neumann*, 2001; *Hansteen et al.*, 1998; *Klügel et al.*, 1997; *Schwarz et al.*, 2004]. Previous studies have shown that barometric conditions of magma storage and ascent can be estimated from densities of fluid inclusions trapped in phenocrysts and xenoliths [e.g., *Zanon et al.*, 2003; *Zanon and Nikogosian*, 2004; *Frezzotti and Peccerillo*, 2004; *Peccerillo et al.*, 2006; *Klügel et al.*, 2005].

[5] Studies on the magmatism of the Azores islands focused on the geochemical characterization of the mantle source [e.g., *Beier et al.*, 2008, 2010; *Elliott et al.*, 2007; *Claude-Ivanaj et al.*, 2001; *França et al.*, 2006; *Millet et al.*, 2009; *Moreira et al.*, 1999; *Schaefer et al.*, 2002; *Turner et al.*, 1997; *Widom et al.*, 1997; *Widom and Farquhar*, 2003]. Little is known about the shallow evolution of magmas in central eruptive systems and associated rift zones [*Self and Gunn*, 1976; *Métrich et al.*, 1981; *Beier et al.*, 2006; *Snyder et al.*, 2004; *Snyder et al.*, 2007; *Widom et al.*, 1992; *Widom et al.*, 1993]. The few existing barometric data are from the islands of Pico [*França et al.*, 2006] and Corvo [*Larrea et al.*, 2012], and the volcanoes of Sete Cidades and Agua de Pau, in the island of São Miguel [*Mattioli et al.*, 1997; *Renzulli and Santi*, 2000; *Beier et al.*, 2006]. A first attempt to define the evolution history and the different ascent paths of magmas from the fissure zones and a central volcano has been recently proposed for the Island of Faial [*Zanon et al.*, 2013].

[6] In this study, barometric data were obtained through the microthermometric study of the fluid inclusions hosted in the lavas and xenoliths from Pico and Faial, following the approach of *Zanon et al.* [2003]. These two islands are the emerged tops of a larger volcanic edifice, resulting from the interplay of fissural volcanism and eruptions from central volcanoes. The style and typology of magmatism is apparently linked to the interaction between the activity of normal fault systems with the main regional transextensional trend. The present data provide the first evolutionary model of magma flow and storage beneath these two islands. This model outlines how the interplay between tectonics and magma supply rate influenced the ascent and ponding of mafic magmas at depth, and the geometry of the plumbing system beneath the different volcanic systems.

2. Geological Background

[7] The Azores archipelago consists of nine main islands and several islets located in the Atlantic Ocean and extends from northeast to southwest, between latitudes 37°N and 40°N (Figure 1). Magmatism in this area presumably started in the lower Miocene [*Luis and Miranda*, 2008], with the formation of a submarine plateau. The latter is crossed by important tectonic structures: the Mid-Atlantic Ridge, the East Azores Fracture Zone and the Terceira Rift. *Georgen and Sankar* [2010] reviewed the geodynamic importance of these structures and on their relationship with the magmatism in the Azores area.

[8] The islands are the emerged tops of larger volcanic elongated ridges that crop up from the
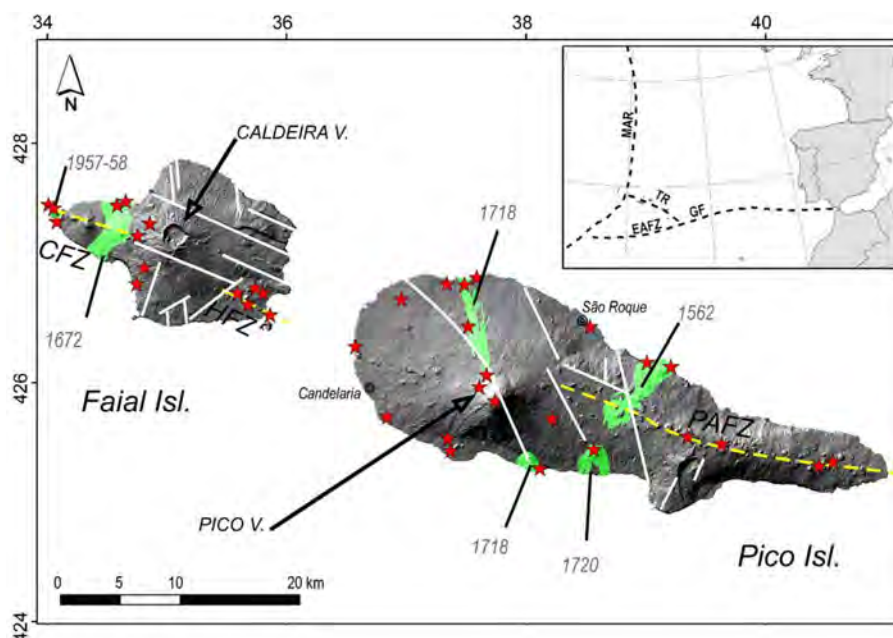
Figure 1. Digital Elevation Model of the islands of Faial and Pico, showing the principal geographic features, historic eruptions, main faults (in white), and fissure systems (yellow dashed lines). Tectonic data are from *Madeira* [1998] and *Madeira and Brum da Silveira* [2003]. Fissure zones are labeled as follows: CFZ—Capelo Fissure Zone; HFZ—Horta Fissure Zone; PAFZ—Planalto da Achada Fissure Zone. Stars indicate sampling sites. Coordinates reported in the grid must be multiplied by 10,000. The inset shows a general location map of the Azores archipelago and the main geostructural lineaments. Acronyms are as follows: MAR—Mid-Atlantic Ridge; TR—Terceira Rift; EAFZ—East Azores Fracture Zone; GF—Gloria Fault.

submarine plateau; their subaerial eruptions occurred since at least 7.1 Ma ago in the island of Santa Maria [*Abdel-Monem et al.*, 1975]. A temporal gap of about 5 Ma separates the formation of these rocks from those cropping out in Flores island, while all the other islands were apparently formed at least 1.3 Ma ago [*Caniaux*, 2005]. Several eruptions have taken place since the colonization of the archipelago (i.e., around A.D. 1427—*Zbyszewski*, 1963) in the islands of Faial, Pico, São Jorge, Terceira and São Miguel. The last eruption was submarine and occurred in 1998–2001, ~20 km offshore Terceira.

[9] The islands of Faial and Pico developed along a WNW-ESE alignment and formed in a period of 850 ka [*Hildenbrand et al.*, 2012] and about 240 ka [*Madeira and Brum da Silveira*, 2003], respectively. These islands originated from the interplay between fissure volcanism and eruptions from composite volcanoes. Fissure volcanism occurred along a few-kilometer-long subparallel clusters of fractures, whose alignment is generally similar to that of the other nearby islands (Figure 1). Lava accumulation along these fractures caused the formation of volcanic ridges that consist of several rows of cinder cones. In the island of Faial, the

most developed system is the Capelo Fissure Zone in the western part of the island, where it climbs along the western slope of the central volcano of Caldeira. Its activity, which started presumably about 6 ka ago, includes also the eruptions of 1672 and 1957–1958. The Horta Fissure Zone, in the southeastern part of the island is less extended (only ~4 km long). The activity of this system has not been dated, however the presence of 16 ka old pyroclastic fallout generated by the Caldeira Volcano, covering the Horta lavas, excludes magmatic activity during the Holocene. Poorly evolved magmas, from basalt to hawaiites, poured out from these two fissure zones [*Métrich et al.*, 1981; *Zanon et al.*, 2013].

[10] The central volcano of Caldeira is a broad edifice topped by a deep circular caldera. Its main morphological feature is the presence of the Pedro Miguel graben, which dissects the whole edifice from WNW to ESE. This edifice rises where N150° striking tectonic systems interacted with fissure systems and it is possible that this interaction favored the formation of short-lived and shallow-level magma reservoirs, leading to the establishment of a centralized feeding conduit or a series of closely spaced feeding dykes [*Miranda et*

al., 1998]. Basalt-to-trachyte magmas [*Métrich et al.*, 1981; *Zanon et al.*, 2013] were erupted by this volcano starting from ~120 ka ago [*Hildenbrand et al.*, 2012], and its last eruptive event took place ~1.2 ka ago [*Madeira*, 1998].

[11] Pico is an elongated island characterized by the presence, in its western part, of the steep Pico Mountain (2300 m asl). This 240 ka old central volcano [*Chovelon*, 1982] has an almost perfectly circular base and numerous lateral vents which are either isolated or arranged along small radial fissures that punctuate its flanks. Two areas of partial sector collapses are located north and south of the summit area. On its summit, there is a small and young caldera, partially filled with the lavas emitted by a steep and tall nested hornito. A well-evident NW-SE trending fault intersects the whole edifice, passing through the summit caldera. This fault drove magma toward the surface during the A.D. 1718 eruption. Another eruption from this volcano occurred along a more southeasterly located radial fracture, in A.D. 1720.

[12] East of the Pico Volcano, there is the Planalto da Achada Fissure Zone. This structure is similar to the Capelo Fissure Zone and follows the same geographic direction, but it is considerably longer (~30 km). About 170 cinder cones, some of which have a considerable size, constitute this ridge. The oldest lava flow unit dated here is 230 ka old [*Chovelon*, 1982], but magmatism continued until the last eruption in 1562.

[13] Both the Pico Mountain and the Planalto da Achada Fissure Zone erupted poorly evolved magmas, whose composition ranges from basalt to hawaiites. The only exception regards a mugearite erupted in 1718 [*França et al.*, 2006].

3. Methods

[14] Activation Laboratories (Canada) performed 24 whole-rock analyses of major elements using inductively coupled plasma (ICP). Reproducibility was generally better than 1%. Densities of bulk xenoliths and lava samples were measured making use of a MD 200s electronic densimeter and corrected for porosity. The density resolution was is 0.001 g·cm^{-3}.

[15] Electron microprobe analyses of mineral phases in lava and xenolith samples were obtained with a JEOL JXA 8200 Superprobe, equipped with five wavelength-dispersive spectrometers, Energy Dispersive X-ray spectroscopy (EDS), and cathodoluminescence detectors, (University of Milan). A spot size of 1 μm with a beam current of 15 nA was considered for all the mineral phases, whereas a spot size of 5–7 μm, according to the available surface to be analyzed, and a beam current of 2 nA were applied to glasses. Counting times were 30 s on the peak and 10 s on each background. Natural and synthetic minerals and glasses, used as standards, were calibrated within 2% at 2σ standard deviation. Raw data were corrected applying a Phi-Rho-Z quantitative analysis program. The typical detection limit for each element is 0.01%. All the geochemical data are in the supporting information (Table S3).

[16] Fluid inclusions were studied in 31 lava and six xenolith samples. About 0.5–1 kg of each lava sample was coarsely crushed up to obtain the final grain size of the largest crystal that could be visible at a macro scale. About 150/200 olivines and 100/150 clinopyroxenes were embedded in epoxy and doubly polished up to attain a final thickness of about 120–80 μm. For xenoliths, 100–130 μm thick doubly polished wafers were prepared.

[17] Microthermometry was carried out on a Linkam MDSG600 heating-cooling stage, calibrated according to synthetic fluid inclusion standards of pure CO_2 and H_2O. Melting and homogenization temperatures are reproducible to $\pm 0.1°C$ with heating rates in the range of 0.2–0.5°C/min.

[18] Fluid inclusions were further analyzed with a confocal Labram multichannel spectrometer of Jobin-Yvon Ltd. at the University of Siena (Italy). An Ar$^+$ laser produced the excitation line at 514.5 nm. The Raman intensity was measured with a peltier-cooled carbonate compensation depth (CCD) detector. The beam was focused to a spot size of about 1–2 μm using an Olympus 100$\times$ lens. The scattered light was analyzed using a Notch holographic filter with a spectral resolution of 1.5 cm^{-1} and grating of 1800 grooves/mm. Mineral identification was based on our spectral database [*Frezzotti et al.*, 2012a]. Raman identification of optically "hidden" water (i.e., <10 mole %) in fluid inclusions was performed following the approach described in *Frezzotti and Peccerillo* [2007] and *Frezzotti et al.* [2012b].

[19] The densities of the CO_2 fluid were calculated on the basis of the equations (3.14) and (3.15) of *Span and Wagner* [1996]. Isochores for a pure CO_2 fluid were calculated through the application of the equation of state of CO_2 of *Sterner and Pitzer* [1994], valid up to at least 2000°K and 10

GPa. For CO_2-H_2O inclusions (H_2O:CO_2 ratio = 1:9), densities were calculated on the basis of the equation provided in *Sterner and Bodnar* [1991], after the application of the fluid density correction suggested by *Hansteen and Klügel* [2008]. Isochores were calculated using the software "Fluids" [*Bakker*, 2003]. The microthermometric data are shown in the supporting information (Table S4).

4. Description of the Samples

[20] Fluid inclusions were studied in the lava flows emitted from both the fissural systems and from the central volcanoes of the islands of Pico and Faial. Most of the samples date back to the Holocene age and were collected from quite well recognizable volcanic units.

[21] All the lavas ranged in composition from basalt to hawaiite and presented different degrees of porphyricity. Three mugearites from the central volcanoes were collected in order to check if the evolution of magma was associated to changes in the feeding systems. We also carefully examined the ultramafic xenoliths found in some lava flows.

4.1. Central Volcanoes

[22] On the slopes of the central volcano of Pico we collected 16 samples from recent lava flow units, issued from isolated vents far from the summit cone, or from vents located along radial fissures connected to the main feeding system. One lava sample issued from the summit cone was collected on the southwestern rim of the caldera. All samples except one were younger than 40 ka (supporting information, Table S1).

[23] Most of these samples had a very high crystal content and were macroscopically characterized by the presence of a large proportion of mafic phenocrysts (Ø 1.5–6.0 mm) and megacrysts (up to 25 mm in length), totaling between 25 and 70% in volume. Plagioclase was sometimes present only as phenocrysts of 8–12 mm in size. Megacrysts were commonly either widespread inside lava flows or concentrated in discontinuous layers or lenses. In a single case, they appeared as patches of a dense network of euhedral and equidimensional crystals, physically linked to one another. The historical lavas had a variable degree of porphyricity. Those collected from the southern vents of the 1718 eruption were macroscopically characterized by the presence of some megacrysts of oli-

vine and clinopyroxene and few phenocrysts. Lavas issued from the northwestern vents showed no megacrysts, but, on the contrary, there were numerous phenocrysts of plagioclase, olivine, clinopyroxene and many gabbroic and cumulitic xenoliths. The lava emitted in 1720 was poorly porphyritic with few plagioclases and mafic phases.

[24] In Faial, the whole surface of the central volcano of Caldeira exhibited a thick pyroclastic cover produced during its Holocene activity. Two lavas were therefore collected from rare accessible outcrops along the coast and from some gullies on the southeastern flank of the volcano. These samples were poorly porphyritic lavas issued during a period starting from 120 ka ago. The first one showed similar characteristics to the southern historic lavas from Pico, while the second rock had only few macroscopic plagioclases.

4.2. Fissure Systems

[25] All the lavas and pyroclasts collected from all the fissure zones had in general very similar characteristics, i.e., they were poorly porphyritic with a phenocrysts content (olivine, clinopyroxene ± plagioclase) amounting to less than 20% in volume and were devoid of megacrysts.

[26] The bulk rock composition ranged from basalt to hawaiite. Some lavas with a higher crystal content were collected only in the Capelo Fissure Zone area, where numerous phenocrysts of olivine were scattered over the flow and did not form any evident accumulation texture. In any case, only a lava sample that contained some xenoliths had a crystal content comparable to that of the highly porphyritic lavas from Pico central volcano.

[27] In the island of Pico, seven samples were collected along the axial ridge of the Planalto da Achada Fissure Zone and from the vertical cliff on the northern coast, where a succession of thin lavas is capped with the A.D. 1562 flow. With the exception of a single sample, which is older than 50 ka, all the other rocks are of the Holocene or historic.

[28] In the island of Faial eight rocks collected along the fissure zones come from scoria cones or associated lava flows and were representative of the whole activity which developed there. The samples from Capelo Fissure Zone are younger than 6 ka, those from Horta Fissure Zone are older than 11 ka.

4.3. Ultramafic Xenoliths

[29] Ultramafic xenoliths were only found in lavas from Planalto da Achada Fissure Zone, in Pico and Capelo Fissure Zone, in Faial. In both cases, these lava flow units cropped out at the morphological boundary between the central volcano and the fissure zone. The flow from Planalto da Achada Fissure Zone (Pico Isl.) is older than 50 ka. It crops out at the base of the northern cliff, covered by the A.D. 1562 lava, at a distance of ~15 km from the crater of the central volcano. However, its source vent can be reasonably located close to that of 1562, at a short distance from the eastern slopes of the central volcano, i.e., at the boundary between a central volcano and a fissure zone. The host lava was poorly porphyritic and contained olivines and clinopyroxenes. The size of xenoliths did not exceed 3–4 cm.

[30] The flow from Capelo Fissure Zone (Faial Isl.) was a crystal-rich lava which cropped out on the northern coastal cliff. This lava is not dated; however, due to the existing dating of the Capelo rocks, we can assume that this flow is younger than 6 thousand years. Xenoliths were compositionally heterogeneous, with the typical size ≥ 20 cm and had either a rounded or an angular shape.

5. Petrographic Characteristics

5.1. Lava and Scoria Samples

[31] All the samples showed the same petrographic and geochemical characteristics. The only difference was represented by the total crystal content that in rocks from fissure zones did not exceed 19% in volume, while in the lavas from the central volcano of Pico, it ranged between 25% and 70% (supporting information, Table S2). These latter lavas, known as ankaramites (i.e., dark porphyritic mafic lavas with a high content of pyroxene and olivine crystals and minor amounts of plagioclase), contained also numerous mafic megacrysts. Lavas of this kind are common on many other islands of the archipelago and have already been described for the islands of Corvo [*Larrea et al.*, 2012] and Faial [*Zanon et al.*, 2013].

[32] Collected samples ranged in composition from basalt to mugearites (Figure 2; supporting information, Table S3) with mineral assemblage constituted by olivine + clinopyroxene ± plagioclase ± oxides. The typical textures were intergranular and intersertal. Rarer hyaloophitic and
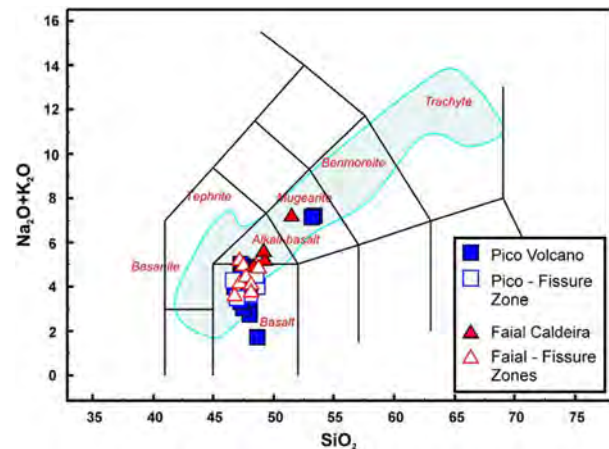

Figure 2. Chemical classification of collected lava samples. Open versus full symbols distinguish samples between central volcanoes and the fissure zones. Light-colored area represents the entire compositional field from existing literature [*Zanon et al.*, 2013; *França et al.*, 2006].

cryptocrystalline textures were also observed (Figure 3a).

[33] Olivine phenocrysts (rarely exceeding 2 mm across) were euhedral, subhedral, and/or skeletal; their core Mg number [Mg# = 100·Mg/(Mg+Fe)] ranged, on average, from 77 to 82 (Figure 4). Only the last tens of microns at their rim were Fe enriched. Euhedral and zoned augites (Wo$_{31-42}$, En$_{31-47}$, Fs$_{3-14}$) were always present in all fissure zones, with the exception of magmas from the Horta Fissure Zone (Faial Isl.), where their presence was rarer. Their Mg# values ranged from 72 to 86. The negative correlation between Ti and Si evidenced in the diagram of Figure 5a, indicated the occurrence of a common crystallization path for all the samples collected. The Al^{IV}/Al^{VI} ratio decreased irregularly with titanium, indicating different and variable pressures of crystallization of clinopyroxenes from microphenocrysts to megacrysts [*Wass*, 1979] (Figure 5b). Plagioclase was ubiquitous in all fissure zones while scarce or absent in the central volcano of Pico. Crystals were typically euhedral, tabular and with oscillatory or reverse zoning and with composition from bytownite to labradorite [*França et al.*, 2006; *Zanon et al.*, 2013].

[34] Olivines, clinopyroxenes and plagioclases, plus ilmenites or titanomagnetites or both, commonly represented microphenocrysts. Amphibole (Ø ≤ 2.5 mm) was present in the lavas emitted during the A.D. 1718 eruption from the northern segment of the fissure. Apatite was frequently found intimately associated with clinopyroxenes and/or
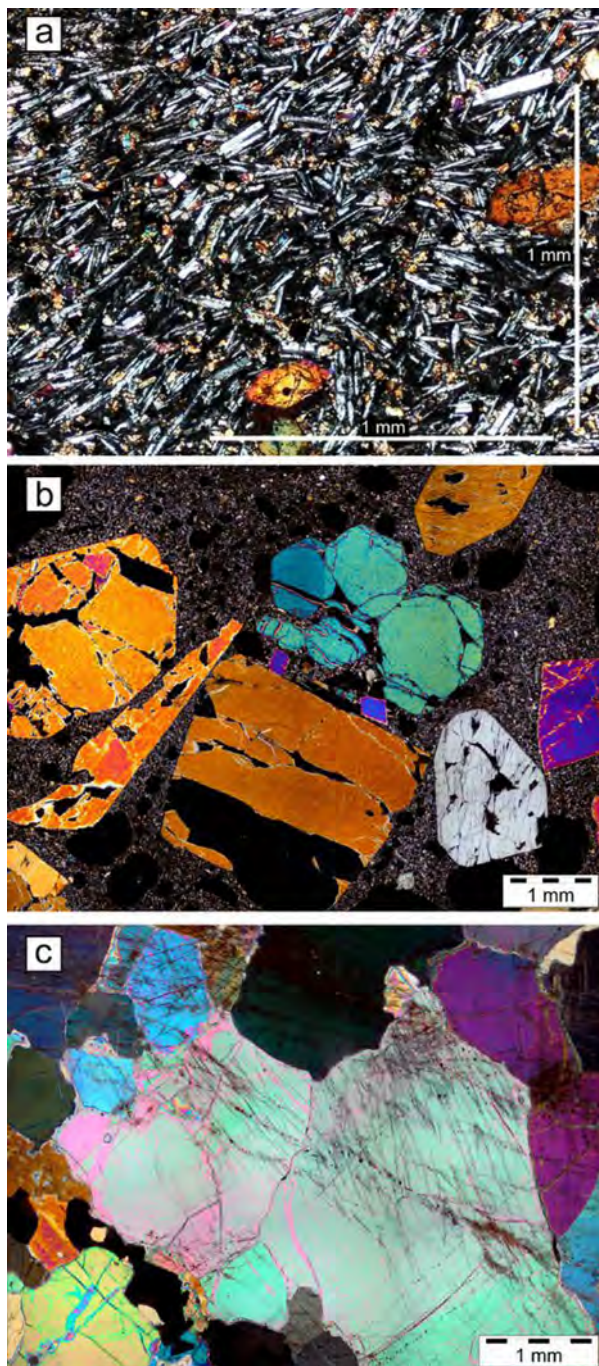
Figure 3. Microphotographs of representative samples. (a) Poorly porphyritic lava of the Horta Fissure Zone, showing two small and partly iddingsitized olivine dispersed among plagioclase microphenocrysts. (b) Highly porphyritic lava sample from the Pico summit cone. It is evident the presence of large euhedral megacrysts of olivine and clinopyroxene. (c) Wherlite sampled from a poorly porphyritic lava of the fissure zone of Pico. The presence of numerous trails of fluid inclusions at the centre of the main is perfectly visible at the centre of the clinopyroxene.

amphiboles. Nepheline was occasionally found in some basalts from Pico Volcano.

[35] The megacrysts of olivines and clinopyroxenes (Figure 3b) were commonly euhedral or subhedral or anhedral, and showed disequilibrium features, such as reaction rims and embayments. It was sometimes very difficult to discriminate between phenocrysts and megacrysts especially for olivines, due to overlapping compositions and crystals size.

[36] A comparison was made between the forsterite content (Fo) in phenocrysts and in megacrysts and the composition of olivines in equilibrium
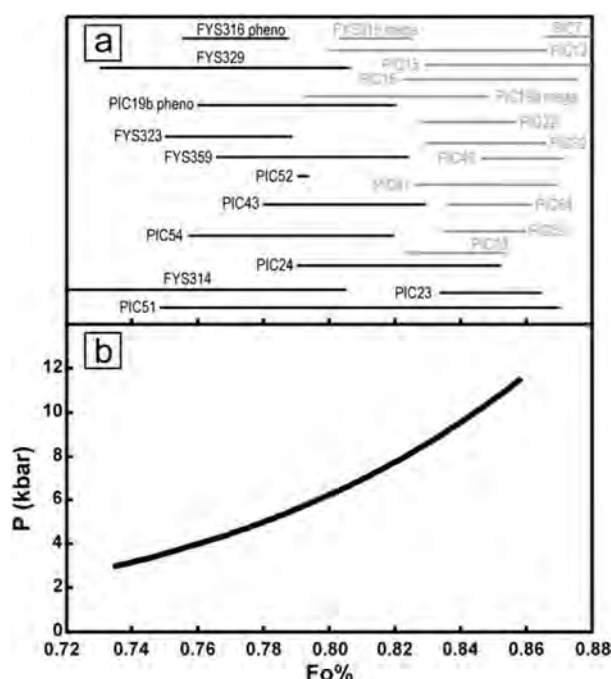

Figure 4. Comparison between the theoretical conditions of olivine crystallization and the measured forsterite content. (a) The variation of forsterite of megacryst (in gray) and of phenocrysts (in black), hosted in various samples of the two islands. (b) The black curve represents the value of forsterite in equilibrium with coexisting silicate melt at various pressures. This curve was simulated in absence of water and under the QFM buffer, with MELTS software [*Ghiorso and Sack*, 1995], starting from a primary melt composition of Faial Island, recalculated from the sample Fys 301, a poorly porphyritic basalt from Horta Fissure Zone (Faial Isl.), already described in *Zanon et al.* [2013]. The primary melt was recalculated after equilibrating the sample composition with Fo89, using the geothermometers of *Lee et al.* [2009]. The resulting conditions of melting were used as input for fractional crystallization simulations (i.e., 1450°C and 25 kbar). The segment of the liquid line of descent shown is relative to the lithosphere thickness (41.9 km) simulated beneath the island of Faial [*Dasgupta et al.*, 2010].
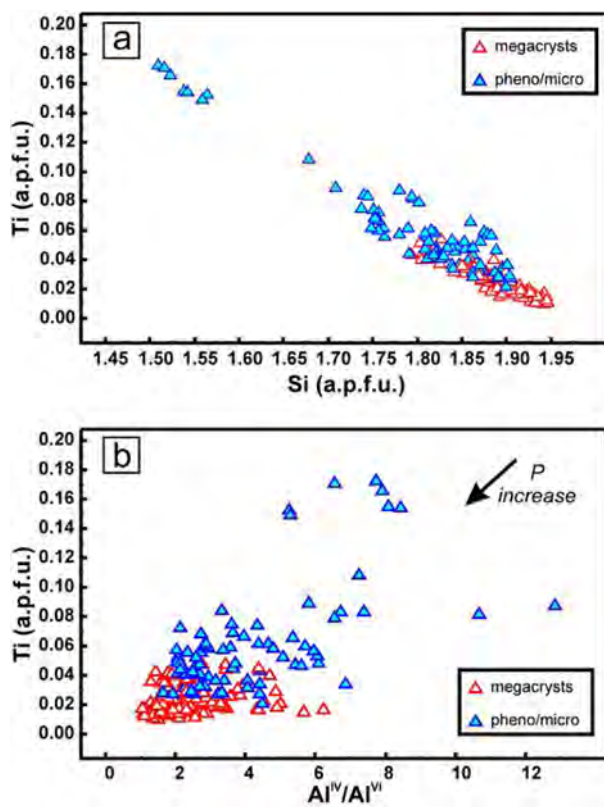
Figure 5. (a) The variations of the Ti in clinopyroxenes of the two dimensional classes are negatively correlated with Si, and form a single trend. This relationship indicates a continuous variation in the crystallization pressure of clinopyroxene [*Wass*, 1979]. (b) Data of Al^{IV}/Al^{VI} versus Ti in the megacrysts of clinopyroxenes in lavas of the central volcano of Pico are poorly variable, while corresponding variations in poorly porphyritic lavas are wider. This indicates that the larger crystals in the highly porphyritic lavas were generated deeper than the smaller ones in the poorly porphyritic lavas. A.p.f.u. stands for Atoms por Formula Unit.

along the liquid line of descent of a recalculated primitive magma composition (Figure 4). Fo was generally higher in megacrysts than in phenocrysts (Figure 4a). However, many phenocrysts also showed disequilibrium conditions with the melt. For this reason, both of them should be considered as "antecrysts" [*Davidson et al.*, 2007], i.e., crystals, which may have formed from a different and more primitive magma than the present host.

[37] Similar considerations were made for clinopyroxenes. Both megacrysts and phenocrysts followed the same evolution path (Figure 5a) and were therefore comagmatic. However, Mg# in megacrysts was higher and less variable (i.e., 79–90) and the variation of the Al^{IV}/Al^{VI} ratio with Ti was limited, which evidenced higher pressure conditions during clinopyroxene crystalliza-

tion (Figure 5b) and made it possible to consider also those crystals as antecrysts. However, the parental link between antecrysts and phenocrysts was not relevant for the purposes of the present work; therefore, in the following discussion, we continued to distinguish megacrysts from phenocrysts.

[38] Mugearites were subaphyric with trachytic texture and phenocrysts assemblages constituted by numerous oligoclase-to-Na-sanidine feldspars (Ø > 4 cm), rare olivines (Ø > 0.15 cm) (Fo_{57-60}) and kaersutite amphiboles. The same phases were present as microphenocrysts together with clinopyroxene, apatite, and oxides (both ilmenite and titanomagnetite).

5.2. Ultramafic Xenoliths

[39] Ultramafic xenoliths were coarse-grained lithologies made up of olivine, clinopyroxene, orthopyroxene, and spinel in various amounts (Figure 3c). Plagioclase and plagioclase-and-amphibole-bearing lithologies were also frequent but have not been described here, since they did not contain fluid inclusions. Mantle xenoliths consisted of three harzburgites from Pico, and one websterite and one wherlite from Faial.

[40] All peridotites showed porphyroclastic to equigranular textures, where olivine and orthopyroxene grains were present as large porphyroclasts (up to 4 mm) and polygonal grains typically < 1 mm. Clinopyroxene was present as polygonal grains in the wherlite and as interstitial grains in harzburgites. Spinel was interstitial (up to 0.5 mm in diameter) or present as inclusions in olivine. Plagioclase was absent; all studied xenoliths equilibrated in the spinel stability field.

[41] Olivine was the dominant phase in all peridotite samples. In harzburgites, it had Mg# ranging from 88 to 90.5, NiO contents ranging from 0.26 to 0.47 wt% and low CaO (<0.17 wt%) and Cr_2O_3 (<0.07 wt%). In harzburgites, orthopyroxene showed higher Mg# than olivine (91–92), high Cr_2O_3 (0.74–0.48 wt%), and low Al_2O_3 (1.56–2.27 wt%) and TiO_2 (<0.13 wt%). Clinopyroxene had also very high Mg# (0.91–0.93), and spinel was Cr rich. In the websterite and in the wherlite Mg# of both olivine and orthopyroxene were between 87 and 88, while slightly higher in clinopyroxene (Mg# = 89–90).

[42] Based on their mineral chemistry, harzburgites from Pico were interpreted as fragments of upper mantle, which underwent partial melting

processes. These were similar to ultrarefractory mantle xenoliths previously reported from São Miguel [*Simon et al.*, 2008]. In contrast, the pyroxenite and the wherlite from Faial had compositions that are more fertile and appeared to represent melts crystallized or cumulated at mantle depth, but not necessarily in a magma chamber.

6. Study on the Fluid Inclusions

[43] In all the samples the fluid contained in the inclusions was rich in CO_2. The distribution of fluid inclusions varied considerably among the samples. In general, they could be frequently found in ultramafic xenoliths, but they were found in ~10–20% of megacrysts of olivine, whereas they were scarce in ~1% of phenocrysts. They were also found in ~5% of clinopyroxene, both megacrysts and phenocrysts, and in some plagioclase phenocrysts.

6.1. Petrographic Analysis

[44] On the basis of their textural characteristics, two populations of fluid inclusions were observed. Early carbonic inclusions (Type I) were either isolated inclusions or in small and spatially defined clusters, located both inside the grains and at its boundaries (Figure 6a). This kind of inclusions was rarely found in few olivine and clinopyroxene grains in highly porphyritic lavas of Pico Volcano and in a single olivine from a poorly porphyritic lava of the Horta Fissure Zone (Faial Isl.). The inclusions were generally rounded or rarely negative crystal shaped, with a size ≤20–30 μm. At room temperature, Type I inclusions were single phase (L) or might contain a vapor bubble (L+V). Their texture often showed evidences of partial density re-equilibration, such as haloes of tiny fluid inclusions (Ø < 1 μm) surrounding a main inclusion cavity, and/or short cracks radiating from the microcavity [*Viti and Frezzotti*, 2000, 2001]. A few inclusions, contained in a single olivine megacryst from a single sample of the volcano of Pico hosted a tiny (Ø ≤ 5 μm) Mg-calcite [(Ca,Mg)CO₃—Figure 7a], identified by Raman microspectroscopy by its diagnostic vibrations at 714 and 1087 cm^{-1} [*Frezzotti et al.*, 2012a]. In another group of inclusions of the same samples, the presence of dypingite (Mg₅[(OH)(CO3)₂]₂·5H₂O [*Frost et al.*, 2008] was identified for its main Raman vibration at 1122 cm^{-1}—Figure 7b.

[45] Late carbonic fluid inclusions (Type II) were dominant in all the studied samples, where they
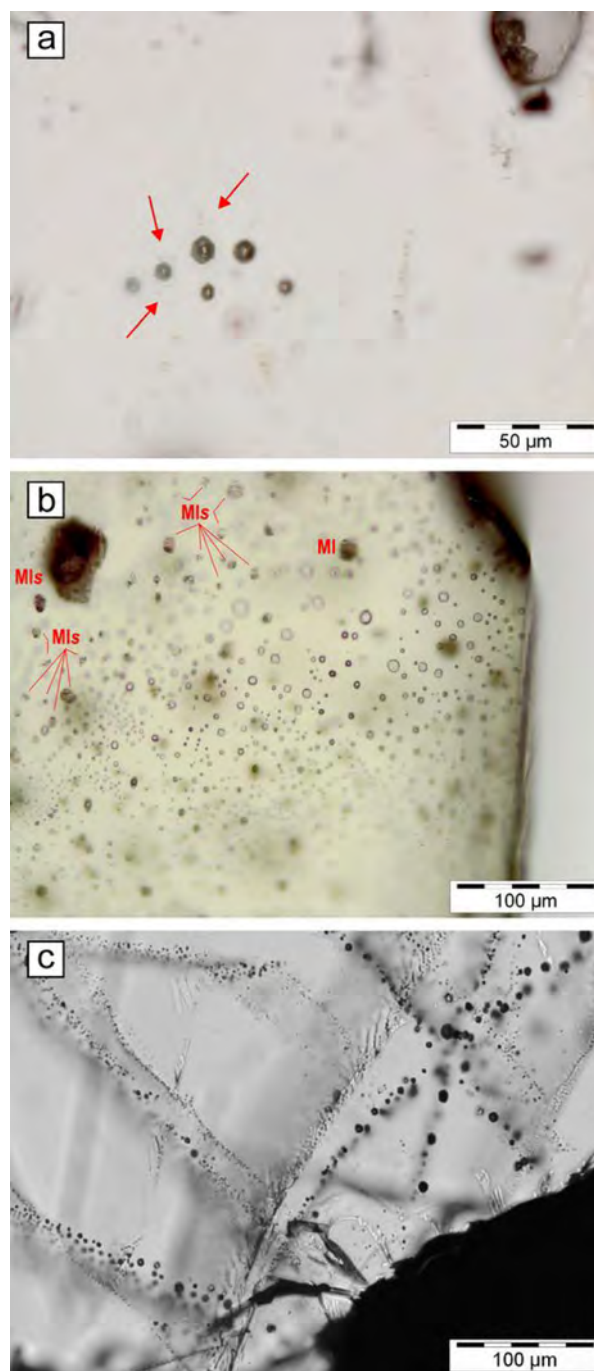

Figure 6. Photomicrographs of the different types of fluid inclusions hosted in olivines, and their textures. (a) Olivine from the 1718 eruption in Pico Island, showing a cluster of Type I fluid inclusion with decrepitation features (halo of tiny bubbles), marked by red arrows. (b) Olivine from a highly porphyritic lava from the central volcano of Pico, showing numerous Type II diffuse fluid inclusions, coexisting with several silicate melt inclusions of different size. (c) Olivine from a dunite fragment from Faial Island, showing various trails of tiny (2–15 μm) Type II fluid inclusions.
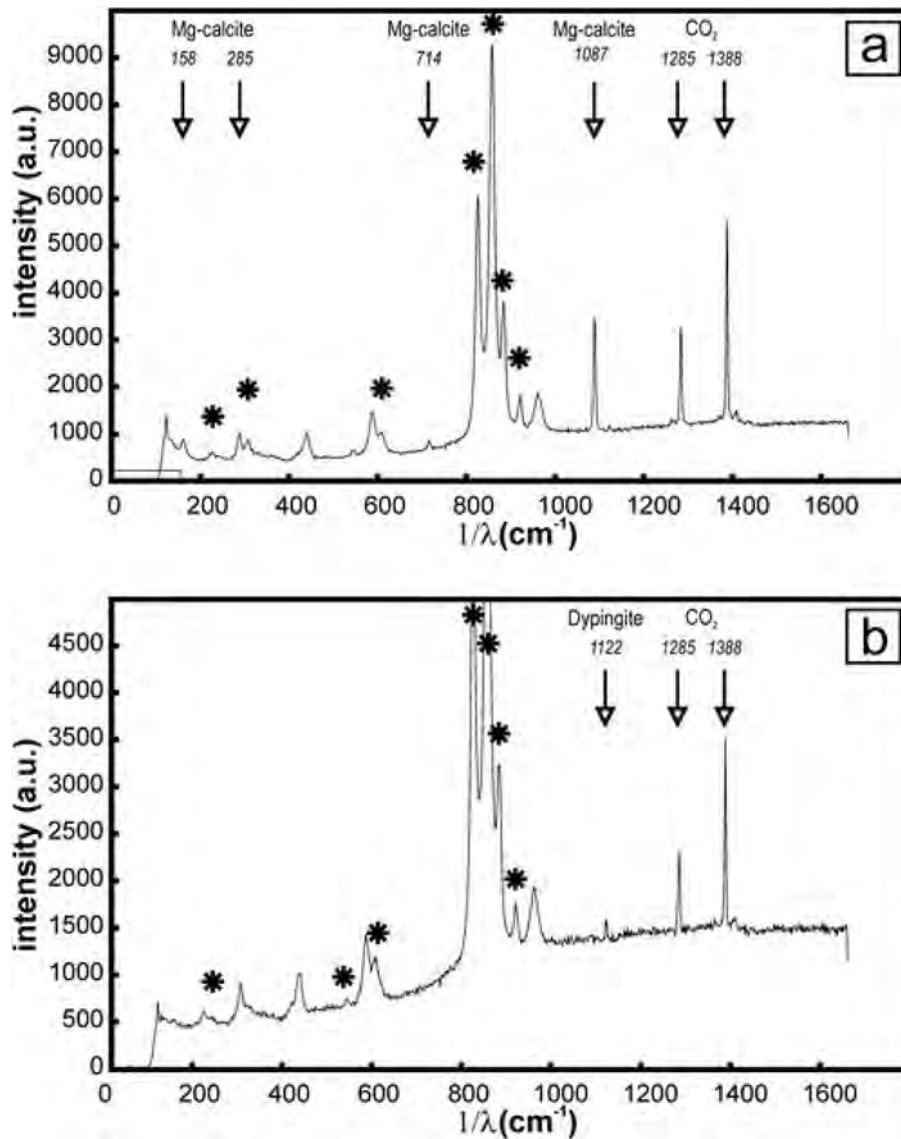
Figure 7. Raman spectra of crystalline phases found inside Type I fluid inclusions (three acquisitions for 30 s band area integration, with a laser power of 300 mW). The main vibrations at 1285 and 1388 cm^{-1} are characteristic of CO_2. Raman bands of host olivine are marked with asterisks. (a) Peaks of Mg-calcite— $(Ca,Mg)CO_3$. (b) The vibration of the hydrated carbonate dypingite—$Mg_5[(OH)(CO_3)_2]_2\ 5H_2O$.

formed trails of variable length and thickness, which lined completely healed fractures, limited or crosscutting grain boundaries (Figures 6b and 6c). The inclusions were typically $\leq 30\ \mu$m, usually rounded (Figure 6c) or with a negative-crystal shape. At room temperature, Type II inclusions were single phase (L) or two phases (L+V), commonly liquid rich. Many inclusions showed evidence of re-equilibration and coexisted with numerous silicate melt inclusions with a variable size and crystallization degree. These silicate melt inclusions may contain a large CO_2-rich bubble.

6.2. Composition

[46] On cooling, CO_2-rich inclusions froze between -68 and $-92°C$. A further decrease of temperature did not produce any visible phase change. Most of the inclusions melted instantaneously within a temperature interval between 57.1 and 56.4°C with most of the data at 56.6°C. Clathrates were not observed and final homogenization occurred to either the liquid (Th$_L$) or the vapor phase (Th$_V$) at $<31.1°C$. Liquid water was not detected, neither optically nor by Raman spectroscopy, in any of the measured inclusions.

[47] The identification of dypingite by Raman spectroscopy in a few Type I inclusions in olivine megacrysts suggests that some water was originally present in these inclusions, and reacted with the host olivine to form a hydrous carbonate at later stages. The determination of the original water content in Type I inclusions is difficult since the H_2O content of the magma at the time of degassing in not known. Different lines of evidence suggest that a plausible upper limit could be 10 mole % [*Hansteen and Klügel*, 2008]. Water is subordinate in CO_2-H_2O fluids released by basaltic magmas and generally around 10 mole % in magmas from intraplate settings [*Dixon and Stolper*, 1995]. In addition, thermodynamic modeling of the fosteritic olivine—CO_2-H_2O fluid reaction on cooling as inclusions at 0.1 GPa suggests similar water contents, since talc would have formed along with carbonates in CO_2-H_2O inclusions with X_{H2O} higher than 0.1 (Figure 7) [cf. *Frezzotti et al.*, 2012b].

6.3. Density

6.3.1. Xenoliths

[48] Type II inclusions homogenized to liquid phase (Th$_L$; L+V →L) from 10 to 30.4°C (d = 0.70–0.81 g·cm^{-3}). Only one inclusion homogenized to vapor phase (Th$_V$; L+V →V) with Th$_V$ 29.4, corresponding to a density of 0.32 g·cm^{-3}. The histogram of homogenization temperatures shows data from each island (Figure 8). These data formed a polymodal distribution, depending mainly on the re-equilibrated inclusions. A comparison of the densities of the inclusions in the xenoliths of the two islands is shown in Figure 9a.

6.3.2. Poorly Porphyritic Lavas From Fissure Zones

[49] Type II fluid inclusions from both the Capelo (Faial Isl.) and Planalto da Achada Fissure Zones (Pico Isl.) were in olivines and clinopyroxenes and homogenized to the liquid phase from 16.9°C to 30.6°C (d = 0.56–0.81 g·cm^{-3}). Those from olivines of Horta Fissure Zone (Faial Isl.) were both of Type I and Type II. Type I inclusions homogenized to the liquid phase from 20.4 to 28.3°C, corresponding to densities of 0.77 to 0.65 g·cm^{-3}. A few re-equilibrated inclusions gave higher and scattered Th values. Type II inclusions homogenized to the liquid phase within a short interval of temperature (i.e., 20.5–25.4°C), corresponding to densities of 0.71–0.77 g·cm^{-3}. Density values related to inclusions in fissure zones are compared in Figure 9b.

6.3.3. Poorly Porphyritic Lavas From the Caldeira Volcano

[50] The fluid inclusions found at this volcano were only in two olivines and three plagioclases and did not show re-equilibration textures. In olivine, Type I homogenized to the liquid phase from 16.4 to 24.3°C (d = 0.72–0.81 g·cm^{-3}). A single Type I inclusion gave a Th$_V$ of 30.9°C (d = 0.42 g·cm^{-3}). In plagioclase from a mugearite, Type II inclusions homogenized to the vapor phase from 23.1 to 30.9°C (d = 0.22–0.42 g·cm^{-3}; Figure 9).

6.3.4. Highly Porphyritic Lavas From Pico

[51] In all megacrysts of Pico Volcano (both clinopyroxene and olivine) from recent eruptions Type I fluid inclusions were rare and sometimes coexisted with Type II, silicate melt and cubic oxides. Re-equilibration features were common. Homogenization of Type I pure CO_2 fluid occurred to the liquid phase between 28.3 and 31°C (d = 0.52–0.65 g·cm^{-3}). Type I H_2O-CO_2 fluid homogenized to the liquid phase between 24.9 and 31°C, corresponding to a corrected density of 0.54–0.74 g·cm^{-3} (Figure 9c).

[52] Type II CO_2 fluid inclusions were found both in xenocrysts and in phenocrysts and homogenized to the liquid phase between 23 and 31°C (d = 0.51–0.74 g·cm^{-3}) and to vapor phase between 28.5 and 31°C (d = 0.32–0.47 g·cm^{-3}).

7. Discussion

7.1. Significance of Fluid Inclusion Data

[53] Fluid inclusions were present in different kinds of crystals, linked to different periods of the volcanism in these islands and to the rocky bodies crossed by the ascending magmas.

[54] The density histograms (Figure 9) showed symmetric or skewed unimodal and bimodal distributions to lower density values related to various extents of fluid inclusions re-equilibration processes. In general, the smaller-size inclusions show the highest density (Figure 10). This kind of inclusion did not undergo re-equilibration, providing useful information on the locations of the magma reservoirs [cf. *Andersen and Neumann*, 2001, and references therein]. Based on the density versus size of inclusion plot (Figure 10) we assume the highest fluid densities as representative for barometric studies.

[55] The ultramafic xenoliths suite preserved the densest inclusions, (about ∼0.86 g·cm^{-3}). The
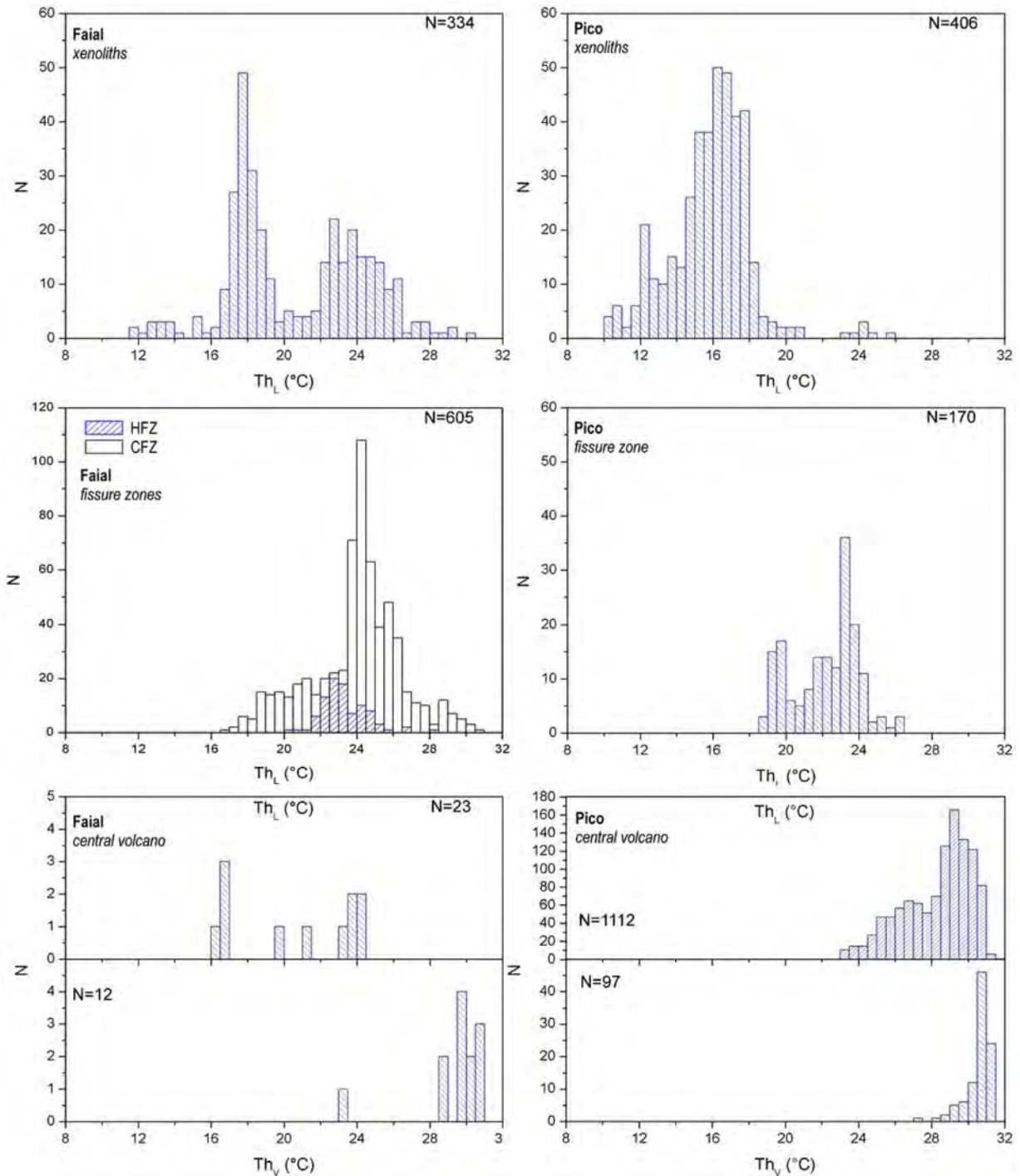
Figure 8. Histograms of the temperatures of homogenization of fluid inclusions from Faial and Pico volcanic systems. The number of the total measurements is reported to the upper left corner of each graph. Only in the case of the two fissure zones of Faial, data are superimposed.

maximum value of CO_2 fluid density in the poorly porphyritic lavas, issued from all the fissure zones, was within the range $\sim$0.77–0.81 g·cm^{-3}. Conversely, in plagioclase maximum density was 0.42 g·cm^{-3}.

[56] Type I H_2O-CO_2 inclusions in highly porphyritic lavas range from $\sim$0.54 to 0.74 g·cm^{-3}.

[57] Barometric information on the magma plumbing system, were obtained from isochore distribution
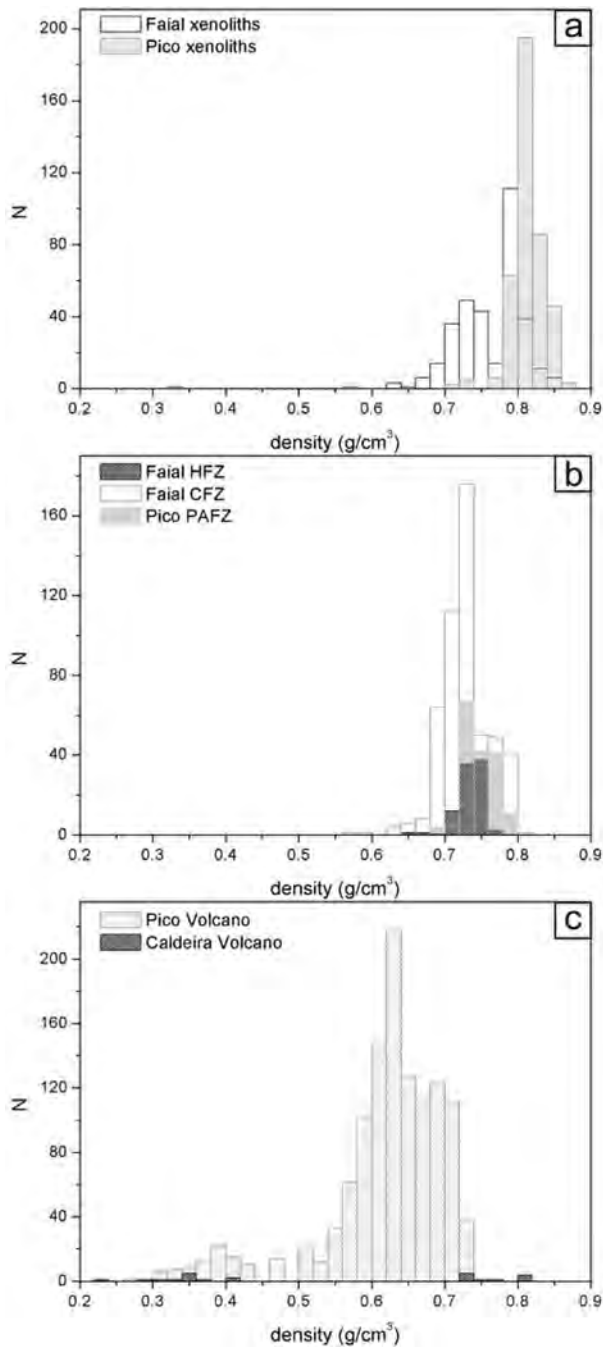
Figure 9. Histograms of the density values found in these inclusions. Data are grouped in the three following classes: xenoliths, poorly porphyritic lavas, and highly porphyritic lavas.
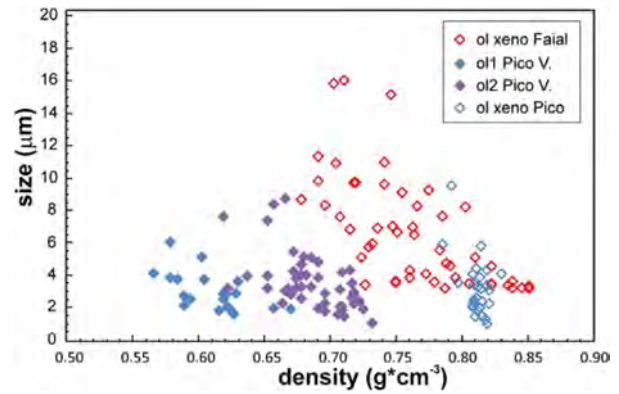

Figure 10. Comparison between inclusions size and the density of the trapped fluid. Measurements refer to various populations of inclusions trapped in different olivine crystals. Partial resetting is evidenced by the existence of various class sizes for all the density values except for the highest.

between the crystallization of olivine and that of clinopyroxene;

[59] 2. Magma ascent was rapid enough to be considered isothermal, i.e., temperatures did not substantially change.

[60] The conditions of clinopyroxene-liquid equilibration were verified according to *Duke* [1976]. When these conditions were lacking, a thermometer based on the composition of the clinopyroxene was used. The values attained mainly concerned highly porphyritic lavas from Pico and ranged
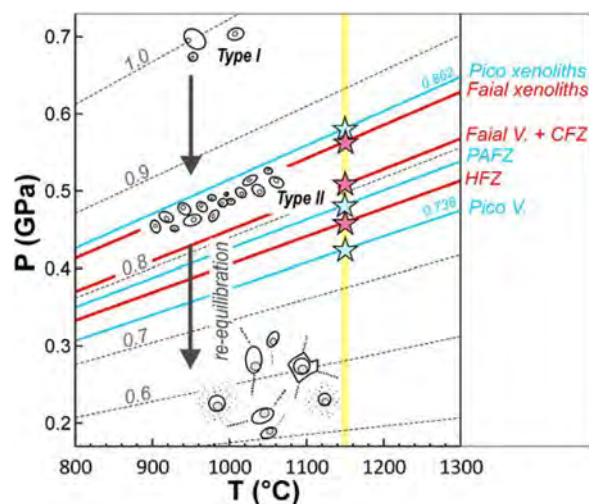
in the P-T space, at the assumed trapping temperature, as shown in Figure 11. Trapping temperature were calculated using the geothermometer based upon the clinopyroxene-liquid equilibrium [*Putirka*, 2008] and assuming that:

[58] 1. The resulting temperatures were representative of the melt evolution stage occurring

Figure 11. Summary outline of the method used to get barometric information. The blue and green stars indicate the intersection of the isochores of the various volcanic systems of Pico and Faial, respectively, with the calculated eruptive temperature of 1150°C. The variations of the textural characteristics of the inclusions, with the occurrence of decrepitation (re-equilibration) are also shown. Acronyms as from Figure 1.
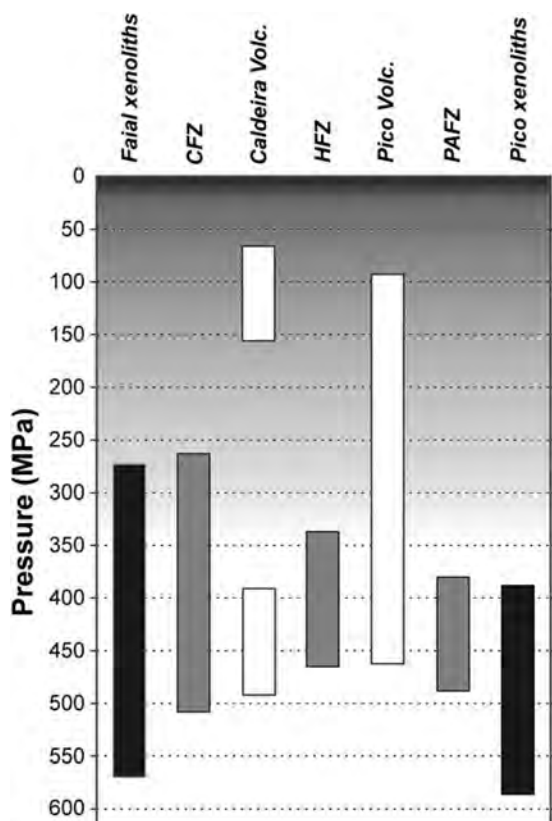
Figure 12. Arrangement of the storage systems beneath each of the volcanic systems in a W-E transect. Deep gray color represents the xenoliths suites of the two islands, intermediate gray color represents the lavas of the various fissure zones and white color represents the lavas of the central volcanoes.

from 1142 to 1240°C. A single value of 1145°C was obtained for poorly porphyritic lavas from Faial, using the clinopyroxene composition (supporting information, Table S5).

[61] Published thermobarometric data reported temperatures from 1100 to 1200°C and pressures ranging from 0.6 to 1.1 GPa for Pico magmas [*França et al.*, 2006]. Faial literature data, based upon the use of a clinopyroxene-melt equilibrium thermometer, reported 1117–1280°C (±10) for poorly porphyritic lavas from fissure zones and 1015°C (±20) for one mugearite [*Zanon et al.*, 2013]. On the basis of this information and in consideration of the data calculated for the highly porphyritic lavas of Pico, a temperature of 1155°C (±15) was assumed for all the poorly porphyritic lavas of the two islands and for the xenoliths contained in them, supposing the existence of a thermal equilibrium between the xenoliths and the host magma. A temperature of 1100°C (±10) was assumed for the mugearites of

Faial. It is worth noting that a difference in temperature of ±10°C does not significantly affect the resulting pressure values, which vary only by ±5 MPa. The resulting scheme of fluid pressures is shown in Figure 12.

[62] To convert barometric data into depths it was necessary to include information on the depth of the crust-mantle transition and make some assumptions on the density of the wall rocks. Detailed geophysical data from the local earthquake tomography indicated a crustal thickness of 12.5 km beneath Faial and from 13 to 14 km beneath Pico [*Matias et al.*, 2007]. Regarding densities, the average values of 2.8 g·cm^{-3} and 3.22 g·cm^{-3} were considered as being representative of the lithologies of the crust and of the shallow mantle respectively. The first value was the average density among 15 samples of basalts from Faial, while the second was the average among 13 samples of ultramafic lithologies from the two islands (see analytical appendix).

7.2. Relative Timing of Crystallization Path and Fluid Trapping

[63] Megacrysts—These large crystals were comagmatic with phenocrysts; however, their compositional and textural features indicated that they formed in an earlier stage of evolution of the magmas of the two islands. They could be either genetically linked to the host magma or not. In any case, this was not relevant for the purposes of the present study. In some cases, these crystals showed textures typical of a solidification front [*Marsh*, 1996]. They hosted both early (Type I) and late (Type II) stage inclusions. Type I inclusions were related to the degassing of the host melt, which these crystals equilibrated with. Type II inclusions were linked to a further degassing phase, not necessarily related to the same magma. All these inclusions re-equilibrated to the same pressure conditions, providing information only about the last ponding stage, before eruption

[64] Phenocrysts—These were fractionated by the carrier magma at a later stage than megacrysts. They also trapped both early and late stages inclusions related to the degassing of the host magma, and give the same barometric information of the megacrysts.

[65] Crystals from xenoliths—Both ultramafic and cumulitic assemblages were present in the mantle beneath these islands. The inclusions they trapped were all of Type II and were related to the
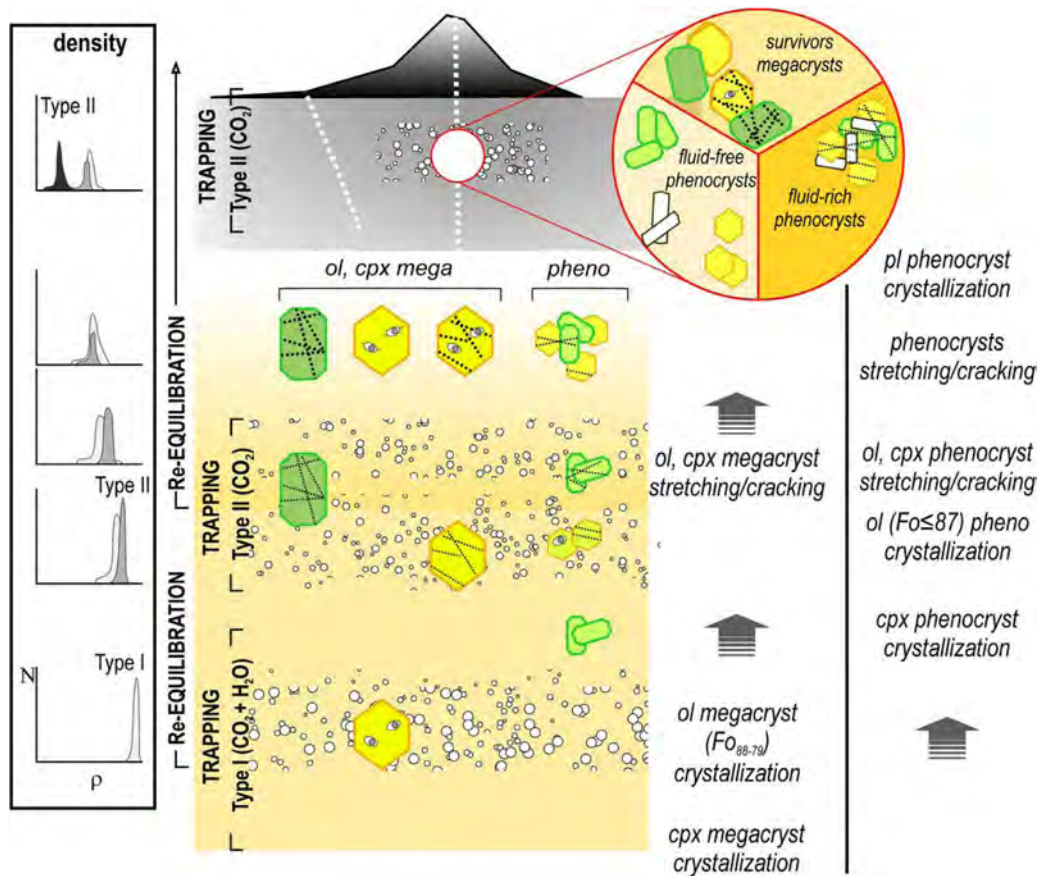
Figure 13. Relationships among process of crystallization of xenocrysts and phenocrysts, occurrence of trapping and re-equilibration of CO_2 inclusions and textures found. The circle represents the various subpopulations of mineral phases that can coexist within the same sample, just prior to ascent through the crust. The two possible pathways evidenced by the dashed lines are suggestive for the central volcano and the fissure zones.

degassing of the carrier magma. The resulting information was related only to the depth at which the magmas ponded at subcrustal depths.

[66] Combining the information obtained from fluid inclusions (textures, densities, relative distribution), petrography (textures and constitution of rocks and minerals) and mineral chemistry of megacrysts and phenocrysts provides unique insights into the magmatological processes that occurred at the mantle-crust boundary (Figure 13).

[67] Three distinct events of fluid trapping occurred at different times. The first event occurred at depth during early crystallization of megacrysts of olivines (Mg# 79–88) and led to the trapping of Type I $CO_2 \pm H_2O$ fluids ($X_{H2O} \leq 0.1$).

[68] While the magma ponded for a long period, the stretching/cracking of olivine and clinopyroxene (both megacrysts and phenocrysts) in the presence of free CO_2 caused the formation of a new generation of fluid inclusions (Type II).

[69] Olivine phenocrysts formed under CO_2 saturation conditions of the coexisting silicate melt, generating Type I inclusions in the olivines contained in poorly porphyritic lavas and in the central volcano of Faial. Decompression gradients caused the complete resetting of these inclusions beneath the fissure zones, as the resulting densities were comparable with those of Type II.

[70] Finally, only a limited number of plagioclases contained in mugearites from the central volcano of Faial recorded the last event of CO_2 fluid trapping/re-equilibration. The low-density Type-II inclusions in some fluids Mg-poor olivines at Pico Volcano possibly result from re-equilibration during slow magma ascent.

7.3. Magma Storage System—The Effect of Tectonics

[71] Overall, our results suggest pressure conditions of trapping and/or re-equilibration,
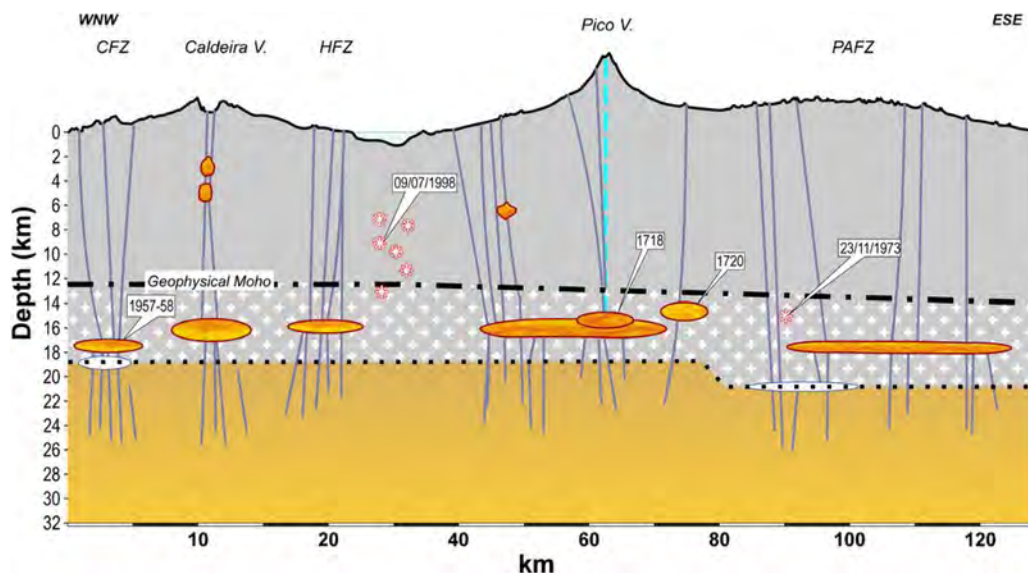
15

Figure 14. Overview of the distribution of the magma reservoirs and the plumbing system of the insular system Pico-Faial, in a WNW-ESE oriented profile. The information resulting from the study of the xenoliths is shown in white. The three dates located close to magma reservoirs are representative for fluid inclusions related to samples of historical eruptions. Blue dotted line indicates the presence of NW-SE main fault in Pico. The black lined and dotted lines indicate the geophysical Moho (data from *Matias et al.* [2007]) and the petrographical Moho, estimated based on fluid inclusions data. Stars indicate the focal depth of historic earthquakes.

characteristic of the very shallow mantle, clearly due to the common occurrence of re-equilibration. A conceptual model of the magma storage process beneath these two islands is shown in Figure 14.

[72] The deepest fluid trapping was recorded only in ultramafic xenoliths at pressures of 570–586 MPa, corresponding to depths of 20 and 21 km, beneath both Faial and Pico respectively. In the poorly porphyritic lavas of the fissure zones and of the central volcano of Faial, trapping/re-equilibrating events occurred at 465–508 MPa (a depth of 16–18 km), whereas at Planalto da Achada Fissure Zone (Pico Isl.), at a maximum pressure of 488 MPa (18 km). The highly porphyritic lavas of Pico Volcano trapped fluids at 463 MPa (16.8 km).

[73] A small intracrustal ponding level beneath the central volcano of Faial is represented by fluid inclusions trapped in plagioclases at 156 MPa (5.7 km). No crustal reservoirs formed during the ascent of magmas beneath the fissure zones.

[74] Geophysical studies located a series of Vp/Vs anomalies beneath the Caldeira Volcano at a depth between 3 and 7 km [*Dias et al.*, 2007], which were interpreted as small crystallized bodies. This shallow-level crustal reservoir was already present at least ~120 ka ago, while the volcano was issu-

ing poorly evolved material. However, the inclusions hosted in the mineral phases of a mugearite suggested that this ponding area played an important role during the geochemical evolution of the magmas. The formation of this long-lived reservoir was probably linked to the important role played by tectonics in this zone of the island [e.g., *Madeira and Brum da Silveira*, 2003]. Recently, *Hildenbrand et al.* [2012] proposed a model of the development and evolution of the islands through successive voluminous magma emissions (edifice building) followed by magmatic quiescence and graben development (edifice collapsing). According to this model, the WNW-ESE regional transtensional tectonics was associated with fissure systems, low degree of magmatic evolution and rapid magma ascent, while the activity of NE-SW and NW-SE system halted the ascent of mafic magmas from depth, favoring the formation of shallow magma storage systems. In this framework, the recent movements of the Pedro Miguel graben [*Hildenbrand et al.*, 2012], the frequent seismicity along a NW-SE direction and the high degree of the evolution of the last products issued by the central volcano during the last 16 ka indicated the end of magmatic activity of the volcano and the onset of a new phase of morpho-tectonic processes.

[75] Only the magmas erupted from the NW sector of the Pico Volcano possibly ponded at crustal depths, at 194 MPa (∼7 km), No other magmas, even those erupted from the main conduit system recorded a trace of this crustal step. For this reason, it is evident that this reservoir was probably short lived and with a limited size. During the A.D. 1718 eruption a mugearite magma was issued from a fissure located NW of the main cone. In the present study, there were no abundant mafic phases available for fluid inclusion study to test for evidence of ponding of the mugearites. We note that a more detailed investigation of fluid inclusions in feldspars could provide this missing information. However, the two analyzed mafic samples, related to the eruptive phases following the emission of mugearite, did not pond inside the crust. This clearly evidenced that mafic magma ascended rapidly through the crust, thus preventing a partial or complete resetting of the already trapped inclusions.

[76] The magma emitted during the following eruption of Pico Volcano (i.e., December 1720) was slightly more primitive than the basalts erupted 2 years before (supporting information, Table S1[1]). This magma followed a different ascent path and did not necessarily pass through the central conduit. Eruptions similar to that of 1720 can be compared to the deep dyke fed from Mt. Etna [*Corsaro et al.*, 2009]. These different ascent paths are thought to be common to many other peripheral cones of this volcano. The NW-SE fault affected the main storage system of Pico, located at a depth of 12.5–16 km, (i.e., well below the mantle-crust boundary found by geophysical methods). The activity rate of this tectonic feature played a major role in the plumbing system of this volcano. It could have led either to the formation of a system of deep-rooted conduits, which favored the rapid ascent of deep-sited magma, or could have temporarily favored the storage of small pockets of magma at crustal levels, promoting the onset of differentiation processes.

[77] The differential displacements caused by *en echelon* faulting in the fissure zones in both the islands of Pico and Faial possibly favored the rapid withdrawal of small volumes of magma stored at the depth of 16–18 km. This means that these faults probably extended at depth and that

they might have crossed the rocks existing beneath the Moho.

7.4. Magma Supply and Consequences for Underplating

[78] To estimate the average magma supply to the central volcano of Pico, to the Planalto da Achada Fissure Zone (Pico Isl.) and to the Capelo Fissure Zone (Faial Isl.), it was necessary to know the average amount of magma emitted during well-delimited periods.

[79] A rough estimation of magma erupted was obtained based on measured lava volumes from specific areas of those volcanic systems [*Nunes*, 1999; V. Zanon, unpublished data, 2013].

[80] If melt production in the mantle did not substantially change between the islands of Faial and Pico [i.e., the same mantle melting degree—*Bourdon et al.*, 2005], it was necessary to hypothesize different time lapses between melting events in these areas: melt production beneath the fissure zones would have occurred sporadically and not continuously, as for the volcano of Pico.

[81] Regarding the second kind of information, i.e., since the ratio of intruded versus extruded magma volumes for oceanic seamounts is between 3:1 and 5:1 [*Crisp*, 1984], the volume of magma intruded beneath Pico Volcano was twice that of the fissure zones (supporting information, Table S6).

[82] Here it followed that:

[83] 1. The different style of tectonic setting and the extent of faults greatly influenced the mantle melting process and the storage of magmas at depth. Beneath the volcano of Pico most of the magmatic arrivals from the source area were almost immediately withdrawn, whereas beneath the fissure zones, magma was stored at the base of the crust, and remained mostly nonerupted.

[84] 2. Accumulated magmas beneath fissure zones crystallized at depth, causing the progressive thickening of the crust and the formation of a transition zone that extended well below the geophysical Moho. Magma ascent through these bodies could only occur when extensional tectonics opened faults at considerable depths. The growth of the transition zone from 12.5 to 18 km developed starting from at least 230 ka (i.e., the oldest age available for the subaerial lavas) beneath the Planalto da Achada Fissure Zone

---

[1]Additional supporting information may be found in the online version of this article.

(Pico Isl.). This caused an average growth rate of 0.024 m/yr.

[85] 3. Crystal mush (ol+cpx) left behind by withdrawn melts was widespread beneath the volcano of Pico. An ascending magma had a high probability to interact with this matter, thus changing its original crystal content and forming highly porphyritic liquids. This working scheme cannot be applied also to the central volcano of Faial, due to the lack of highly porphyritic lavas and to the same crustal thickness of the adjacent fissure zones.

8. Conclusions

[86] According to the existing petrological model of magma generation and evolution beneath the islands of Pico and Faial, mantle melting occurred at a pressure range of 3–4 GPa (∼95–130 km) before migrating toward the surface and crystallizing mafic phases between 0.8 and 1.6 GPa (∼26–50 km) [*Beier et al.*, 2012; *Zanon et al.*, 2013]. Traditional geothermobarometry studies failed to further define the evolutionary conditions of magmas with regard to the depth characteristics of the crust-mantle transition.

[87] The model of magma ponding suggested here through the study of fluid inclusions can fill in the gap and complement the overall model of the genesis and ascent of magmas, providing a detailed picture of the processes occurring at the Moho. Magmas underwent two-step ascent through the lithosphere, separated by a ponding period close to the Moho. During the first ascent phase, mafic magmas began to crystallize olivine and exolved volatiles, which are trapped in growing mineral phases. These ascending magmas ponded, fractionated, re-equilibrated and exolved CO_2 at Moho, possibly saturating the fractures existing in the country rocks. Regional transextensional faulting extended up to these rocks, driving CO_2 up to the surface, as is recognized also in some degassing areas of the archipelago [e.g., *Viveiros et al.*, 2010].

[88] The magma ponding period was long enough to reset completely the first generation of fluid inclusions and to allow further crystallization and carbon dioxide degassing, with the formation of a second generation of fluid inclusions.

[89] Either rapid magma extraction or underplating/fractionation was determined by existing tectonic regime in that area. The formation of highly porphyritic liquids and of ultramafic residua was a different effect of this process. An extreme degree

of crustal thickening could ultimately cause the cessation of volcanic activity. This model may be confirmed by further studies on fossil fissure systems on other islands of the archipelago.

[90] The general interpretation of these data suggest that in volcanic systems the dynamics of the feeding of the eruptions from fissure zones differs from that related to central volcanoes, since it is connected to the existing tectonic regime. This means that in an extensional tectonic environment, central volcanoes and fissure zones, coexisting in the same area, tap completely independent magmatic reservoirs through independent plumbing systems.

[91] The upward migration of magma reservoirs found at La Palma Island [*Klügel et al.*, 2005; *Galipp et al.*, 2006] was not observed here. On the contrary, the storage systems migrated constantly downward due to the increasing difficulty encountered by the drainage of magma and its consequent crystallization at depth. Therefore, the mechanism suggested here seems to be the major responsible factor for the thickening of lithosphere in oceanic islands, in agreement with *Hansteen et al.* [1998].

Acknowledgments

References

Abdel-Monem, A. A., L. A. Fernandez, and G. M. Boone (1975), K–Ar ages from the eastern Azores group (Santa Maria, São Miguel and the Formigas Islands), *Lithos*, *8*, 247–254.

Andersen, T., and E. R. Neumann (2001), Fluid inclusions in mantle xenoliths, *Lithos*, *55*(1-4), 301–320.

Bakker, R. J. (2003), Package FLUIDS 1, Computer programs for analysis of fluid inclusion data and for modelling bulk fluid properties, *Chem. Geol.*, *194*, 3–23.

Beier, C., K. M. Haase, and T. H. Hansteen (2006), Magma evolution of the Sete Cidades volcano, São Miguel, Azores, *J. Petrol.*, *47*, 1375–1411.

Beier, C., K. M. Haase, W. Abouchami, M.-S. Krienitz, and F. Hauff (2008), Magma genesis by rifting of oceanic lithosphere above anomalous mantle: Terceira Rift, Azores,

Geochem. Geophys. Geosyst., *9*, Q12013, doi:10.1029/2008GC002112.

Beier, C., S. Turner, T. Plank, and W. White (2010), A preliminary assessment of the symmetry of source composition and melting dynamics across the Azores plume, *Geochem. Geophys. Geosyst.*, *11*, Q02004, doi:10.1029/2009GC002833.

Beier, C., K. M. Haase, and S. P. Turner (2012), Conditions of melting beneath the Azores, *Lithos*, *144-145*, 1–11.

Belkin, H. E., and B. De Vivo (1993), Fluid inclusion studies of ejected nodules from plinian eruptions of Mt. Somma-Vesuvius, *J. Volcanol. Geotherm. Res.*, *58*, 89–100.

Bonelli, R., M. L. Frezzotti, A. Peccerillo, and V. Zanon (2004), Evolution of the volcanic plumbing system of Alicudi (Aeolian Islands): Evidence from fluid inclusions in quartz xenoliths, *Ann. Geophys.*, *47*(4), 1409–1422.

Bourdon, B., S. P. Turner, and N. M. Ribe (2005), Partial melting and upwelling rates beneath the Azores from a U-series isotope perspective, *Earth Planet. Sci. Lett.*, *239*(1-2), 42–56.

Caniaux, G. (2005), Analyse statistique de la fréquence des éruptions volcaniques aux Açores: Contribution à l'évaluation des risques, *Bull. Soc. Geol. Fr.*, *176*(1), 107–120.

Chovelon, P. (1982), Évolution volcanotectonique des iles de Faial et de Pico, Archipel des Açores-Atlantique Nord, thèse de docteur thesis, 193 pp, Univ. de Paris-Sud, Cent. D'Orsay, Paris.

Claude-Ivanaj, C., J. L. Joron, and C. J. Allègre (2001), 238U–230Th–226Ra fractionation in historical lavas from the Azores: Long-lived source heterogeneity vs. metasomatism fingerprints, *Chem. Geol.*, *176*(1-4), 295–310.

Corsaro, R. A., N. Métrich, P. Allard, D. Andronico, L. Miraglia, and C. Fourmentraux (2009), The 1974 flank eruption of Mount Etna: An archetype for deep dike-fed eruptions at basaltic volcanoes and a milestone in Etna's recent history, *J. Geophys. Res.*, *114*, B07204, doi:10.1029/2008JB006013.

Crisp, J. A. (1984), Rates of magma emplacement and volcanic output, *J. Volcanol. Geotherm. Res.*, *20*(3-4), 177–211.

Dasgupta, R., M. G. Jackson, and C.-T. A. Lee (2010), Major element chemistry of Ocean Island Basalts—Conditions of mantle melting and heterogeneity of mantle source, *Earth Planet. Sci. Lett.*, *289*, 377–392.

Davidson, J., D. Morgan, B. Charlier, R. Harlou, and J. Hora (2007), Microsampling and isotopic analysis of igneous rocks: Implications for the study of magmatic systems, *Ann. Rev. Earth Planet. Sci.*, *35*, 273–311.

Dias, N. A., L. Matias, N. Lourenço, J. Madeira, F. Carrilho, and J. L. Gaspar (2007), Crustal seismic velocity structure near Faial and Pico Islands (AZORES), from local earthquake tomography, *Tectonophysics*, *445*(3-4), 301–331.

Dixon, J. E., and E. M. Stolper (1995), An experimental study of water and carbon dioxide solubilities in mid-ocean ridge basaltic liquids, Part II: Applications to degassing, *J. Petrol.*, *36*(6), 1633–1646.

Duke, J. M. (1976), Distribution of the period four transition elements among olivine, calcic clinopyroxene and mafic silicate liquid: Experimental results, *J. Petrol.*, *17*(4), 499–521.

Eason, D. E., and J. M. Sinton (2009), Lava shields and fissure eruptions of the Western Volcanic Zone, Iceland: Evidence for magma chambers and crustal interaction, *J. Volcanol. Geotherm. Res.*, *186*(3-4), 331–348.

Elliott, T., J. Blichert-Toft, A. Heumann, G. Koetsier, and V. H. Forjaz (2007), The origin of enriched mantle beneath São Miguel, Azores, *Geochim. Cosmochim. Acta*, *71*(1), 219–240.

França, Z. T. M., C. C. G. Tassinari, J. V. Cruz, A. Y. Aparicio, V. Araña, and B. N. Rodrigues (2006), Petrology, geochemistry and Sr–Nd–Pb isotopes of the volcanic rocks from Pico Island—Azores (Portugal), *J. Volcanol. Geotherm. Res.*, *156*(1-2), 71–89.

Frezzotti, M. L., and A. Peccerillo (2004), Fluid inclusion and petrological studies elucidate reconstruction of magma conduits, *Eos Trans. AGU*, *85*(16), 157–159.

Frezzotti, M. L., and A. Peccerillo (2007), Diamond-bearing COHS fluids in the mantle beneath Hawaii, *Earth Planet. Sci. Lett.*, *262*, 273–283.

Frezzotti, M. L., F. Tecce, and A. Casagli (2012a), Raman spectroscopy for fluid inclusion analysis, *J. Geochem. Explor.*, *112*, 1–20.

Frezzotti, M. L., S. Ferrando, F. Tecce, and D. Castelli (2012b), Water content and nature of solutes in shallow-mantle fluids from fluid inclusions, *Earth Planet. Sci. Lett.*, *351-352*, 70–83.

Frost, R. L., S. Bahfenne, and J. Graham (2008), Raman spectroscopic study of the magnesium carbonate minerals artinite and dypingite, *J. Raman Spectrosc.*, *40*, 855–860.

Galipp, K., A. Klügel, and T. H. Hansteen (2006), Changing depths of magma fractionation and stagnation during the evolution of an oceanic island volcano: La Palma (Canary Islands), *J. Volcanol. Geotherm. Res.*, *155*(3-4), 285–306.

Georgen, J. E., and R. D. Sankar (2010), Effects of ridge geometry on mantle dynamics in an oceanic triple junction region: Implications for the Azores Plateau, *Earth Planet. Sci. Lett.*, *298*, 23–34.

Ghiorso, M. S., and R. O. Sack (1995), Chemical transfer in magmatic processes: IV, A revised and internally consistent thermodynamic model for the interpolation and extrapolation of liquid-solid equilibria in magmatic system at elevated temperatures and pressures, *Contrib. Mineral. Petrol.*, *119*, 197–212.

Hansteen, T. H., and A. Klügel (2008), Fluid inclusion thermobarometry as a tracer for magmatic processes, in *Reviews in Mineralogy and Geochemistry*, edited by K. Putirka and F. Tepley, Mineral. Soc. of Am., Chantilly, Virginia.

Hansteen, T. H., A. Klügel, and H.-U. Schmincke (1998), Multi-stage magma ascent beneath the Canary Islands: Evidence from fluid inclusions, *Contrib. Mineral. Petrol.*, *132*, 48–64.

Hildenbrand, A., F. O. Marques, A. C. G. Costa, A. L. R. Sibrant, P. F. Silva, B. Henry, J. M. Miranda, and P. Madureira (2012), Reconstructing the architectural evolution of volcanic islands from combined K/Ar, morphologic, tectonic, and magnetic data: The Faial Island example (Azores), *J. Volcanol. Geotherm. Res.*, *241-242*, 39–48.

Ida, Y. (1995), Magma chamber and eruptive processes at Izu-Oshima Volcano, Japan—Buoyancy control of magma migration, *J. Volcanol. Geotherm. Res.*, *66*, 53–67.

Klügel, A., T. H. Hansteen, and H.-U. Schmincke (1997), Rates of magma ascent and depths of magma reservoirs beneath La Palma (Canary Islands), *Terra Nova*, *9*(3), 117–121.

Klügel, A., T. H. Hansteen, and K. Galipp (2005), Magma storage and underplating beneath Cumbre Vieja volcano, La Palma (Canary Islands), *Earth Planet. Sci. Lett.*, *236*, 211–226.

Klügel, A., S. Schwarz, P. van den Bogaard, K. A. Hoernle, C. C. Wohlgemuth-Ueberwasser, and J. J. Köster (2009), Structure and evolution of the volcanic rift zone at Ponta de São Lourenço, eastern Madeira, *Bull. Volcanol.*, *71*, 671–685.

Larrea, P., Z. França, M. Lago, E. Widom, C. Galé, and T. Ubide (2012), Magmatic processes and the role of antecrysts in the genesis of Corvo Island (Azores Archipelago, Portugal), *J. Petrol.*, *54*, 769–793.

Lee, C.-T. A., P. Luffi, T. Plank, H. Dalton, and W. P. Leeman (2009), Constraints on the depths and temperatures of basaltic magma generation on Earth and other terrestrial planets using new thermobarometers for mafic magmas, *Earth Planet. Sci. Lett.*, *279*, 20–33.

Luis, J. F., and J. M. Miranda (2008), Reevaluation of magnetic chrons in the North Atlantic between 35°N and 47°N: Implications for the formation of the Azores Triple Junction and associated plateau, *J. Geophys. Res.*, *113*, B10105, doi:10.1029/2007JB005573.

Madeira, J. (1998), Estudos de neotectónica nas ilhas do Faial, Pico e S. Jorge: Uma contribuição para o conhecimento geodinâmico da junção tripla dos Açores, PhD thesis, 428 pp., Univ. de Lisboa, Lisbon.

Madeira, J., and A. Brum da Silveira (2003), Active tectonics and first paleoseismological results in Faial, Pico and S. Jorge Islands (Azores, Portugal), *Ann. Geophys.*, *46*(5), 733–761.

Marsh, B. D. (1996), Solidification fronts and magmatic evolution, *Mineral. Mag.*, *60*, 5–40.

Matias, L., N. Dias, I. Morais, D. Vales, F. Carrilho, J. Madeira, J. Gaspar, L. Senos, and A. Silveira (2007), The 9th of July 1998 Faial Island (Azores, North Atlantic) seismic sequence, *J. Seismol.*, *11*(3), 275–298.

Mattioli, M., B. G. J. Upton, and A. Renzulli (1997), Sub-volcanic crystallization at Sete Cidades volcano, Miguel, Azores, inferred from mafic and ultramafic plutonic nodules, *Mineral. Petrol.*, *60*, 1–26.

McLeod, P. (1999), The role of magma buoyancy in caldera-forming eruptions, *Geophys. Res. Lett.*, *26*, 2299–2302.

Métrich, N., H. Bizouard, and J. Varet (1981), Petrology of the volcanic series of Fayal, *Azores, Bull. Volcanol.*, *44*, 71–93.

Millet, M. A., R. Doucelance, J. A. Baker, and P. Schiano (2009), Reconsidering the origins of isotopic variations in Ocean Island Basalts: Insights from fine-scale study of São Jorge Island, Azores archipelago, *Chem. Geol.*, *265*(3-4), 289–302.

Miranda, J. M., et al. (1998), Tectonic setting of the Azores plateau deduced from a OBS survey, *Mar. Geophys. Res.*, *20*, 171–182.

Moreira, M., R. Doucelance, B. Dupré, and C. J. Allègre (1999), Helium and lead isotope geochemistry in the Azores, *Earth Planet. Sci. Lett.*, *169*(1-2), 189–205.

Nunes, J. C. (1999), A actividade vulcânica na ilha di Pico do Plistocénico Superior ao Holocénico: Mecanismo eruptivo e hazard vulcânico, PhD thesis, 357 pp., Univ. dos Açores, Ponta Delgada.

Peccerillo, A., M. L. Frezzotti, G. De Astis, and G. Ventura (2006), Modeling the magma plumbing system of Vulcano (Aeolian Islands, Italy) by integrated fluid-inclusion geobarometry, *petrology, and geophysics, Geology*, *34*(1), 17–20.

Putirka, K. (2008), Thermometers and barometers for volcanic systems, in *Minerals, Inclusions and Volcanic Processes, Reviews in Mineralogy and Geochemistry*, edited by K. Putirka and F. Tepley, pp. 61–120, Mineral. Soc. of Am., Chantilly, Virginia, USA.

Renzulli, A., and P. Santi (2000), Two stage fractionation history of the alkali basalt-trachyte series of Sete Cidades volcano (São Miguel Island, Azores), *Eur. J. Mineral.*, *12*(2), 469–494.

Roedder, E. (1983), Geobarometry of ultramafic xenoliths from Loihi Seamount, Hawaii, on the basis of CO_2 inclusions in olivine, *Earth Planet. Sci. Lett.*, *66*, 369–379.

Ryan, M. P. (1993), Neutral buoyancy and the structure of midocean ridge magma reservoirs, *J. Geophys. Res.*, *98*, 22,321–22,338.

Ryan, M. P. (1994), Neutral-buoyancy controlled magma transport and storage in mid-ocean ridge magma reservoirs and their sheeted-dike complex: A summary of basic relationship, in *Magmatic System*, edited by M. P. Ryan, pp. 97–135, Academic, New York.

Schaefer, B. F., S. Turner, I. Parkinson, N. Rogers, and C. Hawkesworth (2002), Evidence for recycled Archaean oceanic mantle lithosphere in the Azores plume, *Nature*, *420*, 304–307.

Schwarz, S., A. Klügel, and C. Wohlgemuth-Ueberwasser (2004), Melt extraction pathways and stagnation depths beneath the Madeira and Desertas rift zones (NE Atlantic) inferred from barometric studies, *Contrib. Mineral. Petrol.*, *147*(2), 228–240.

Self, S., and B. M. Gunn (1976), Petrology, volume, and age relations of alkaline and saturated peralkaline volcanics from Terceira, Azores, *Contrib. Mineral. Petrol.*, *54*, 293–313.

Sigmundsson, F., et al. (2010), Intrusion triggering of the 2010 Eyjafjallajökull explosive eruption, *Nature*, *468*, 426–430.

Simon, N. S. C., E. R. Neumann, C. Bonadiman, M. Coltorti, G. Delpech, M. Gregoire, and E. Widom (2008), Ultra-refractory domains in the oceanic mantle lithosphere sampled as mantle xenoliths at ocean islands, *J. Petrol.*, *49*(6), 1223–1251.

Snyder, D. C., E. Widom, A. J. Pietruszka, and R. W. Carlson (2004), The role of open-system processes in the development of silicic magma chambers: A chemical and isotopic investigation of the Fogo A trachyte deposit, São Miguel, *Azores, J. Petrol.*, *45*(4), 723–738.

Snyder, D. C., E. Widom, A. J. Pietruszka, R. W. Carlson, and H.-U. Schmincke (2007), Time scales of formation of zoned magma chambers: U-series disequilibria in the Fogo A and 1563 A.D. trachyte deposits, São Miguel, *Azores, Chem. Geol.*, *239*(1), 138–155.

Span, R., and W. Wagner (1996), A new equation of state for carbon dioxide covering the fluid region from the triple point temperature to 1100 K at pressures up to 800 MPa, *J. Phys. Chem. Ref. Data*, *25*, 1509–1596.

Sterner, S. M., and R. J. Bodnar (1991), Synthetic fluid inclusions; X, Experimental determination of P-V-T-X properties in the CO_2-H_2O system to 6 kb and 700 degrees C, *Am. J. Sci.*, *291*(1), 1–54.

Sterner, S. M., and K. S. Pitzer (1994), An equation of state for carbon dioxide valid from zero to extreme pressures, *Contrib. Mineral. Petrol.*, *117*, 362–374.

Turner, S., C. Hawkesworth, N. Rogers, and P. King (1997), U-Th isotope disequilibria and ocean island basalt generation in the Azores, *Chem. Geol.*, *139*(1-4), 145–164.

Viti, C., and M. L. Frezzotti (2000), Re-equilibration of glass and CO2 inclusions in xenolith olivine: A TEM study, *Am. Mineral.*, *85*(10), 1390–1396.

Viti, C., and M. L. Frezzotti (2001), Transmission electron microscopy applied to fluid inclusion investigations, *Lithos*, *55*(1-4), 125–138.

Viveiros, F., C. Cardellini, T. Ferreira, S. Caliro, G. Chiodini, and C. Silva (2010), Soil CO_2 emissions at Furnas volcano, São Miguel Island, Azores archipelago: Volcano monitoring perspectives, geomorphologic studies, and land use planning

application, *J. Geophys. Res.*, *115*, B12208, doi:10.1029/2010JB007555.

Wass, S. Y. (1979), Multiple origins of clinopyroxenes in alkali basaltic rocks, *Lithos*, *12*(2), 115–132.

Watanabe, T., T. Koyaguchi, and T. Seno (1999), Tectonic stress control on ascent and emplacement of magmas, *J. Volcanol. Geotherm. Res.*, *91*, 65–78.

Widom, E., and J. Farquhar (2003), Oxygen isotope signatures in olivines from São Miguel (Azores) basalts: Implications for crustal and mantle processes, *Chem. Geol.*, *193*(3-4), 237–255.

Widom, E., H.-U. Schmincke, and J. B. Gill (1992), Processes and timescales in the evolution of chemically zoned trachyte; Fogo A, São Miguel, Azores, *Contrib. Mineral. Petrol.*, *111*, 311–328.

Widom, E., J. B. Gill, and H.-U. Schmincke (1993), Syenite nodules as a long-term record of magmatic activity in Agua de Pau Volcano, São Miguel, Azores, *J. Petrol.*, *34*, 929–953.

Widom, E., R. W. Carlson, J. B. Gill, and H.-U. Schmincke (1997), Th–Sr–Nd–Pb isotope and trace element evidence for the origin of the São Miguel, Azores, enriched mantle source, *Chem. Geol.*, *140*(1-2), 49–68.

Wilson, L., and J. W. Head (1981), Ascent and eruption of basaltic magma on the earth and moon, *J. Geophys. Res.*, *86*, 2971–3001.

Zanon, V., and I. Nikogosian (2004), Evidence of crustal melting events below the Island of Salina (Aeolian Arc, Southern Italy), *Geol. Mag.*, *141*(4), 525–540.

Zanon, V., M. L. Frezzotti, and A. Peccerillo (2003), Magmatic feeding system and crustal magma accumulation beneath Vulcano Island (Italy): Evidence from fluid inclusions in quartz xenoliths, *J. Geophys. Res.*, *108*(B6), 2298, doi:10.1029/2002JB002140.

Zanon, V., U. Kueppers, J. M. Pacheco, and I. Cruz (2013), Volcanism from fissure zones and the Caldeira central volcano of Faial Island, Azores archipelago: Geochemical processes in multiple feeding systems, *Geol. Mag.*, *130*(3), 536–555.

Zbyszewski, G. (1963), *Les Phénomènes Volcaniques Moderns dans l'Archipel des Açores*, vol. *47*, pp. 227, Comun. dos Serv. Geol. de Portugal, Lisbon, Portugal.